Evaluation of sulfur trioxide detection with online isopropanol absorption method

Jin Xiong[1,2], Yuran Li[1,], Jian Wang[1], Yang Yang[1,2], Tingyu Zhu[1,*]*

1. *Beijing Engineering Research Center of Process Pollution Control, National Engineering Laboratory for Cleaner Hydrometallurgical Production Technology, Institute of Process Engineering, Chinese Academy of Sciences, Beijing 100190, China. E-mail:* jxiong@ipe.ac.cn
2. *University of Chinese Academy of Sciences, Beijing 100049, China*

ABSTRACT

Measurement of the SO_3 concentration in flue gas is important to estimate the acid dew point and to control corrosion of downstream equipment. SO_3 measurement is a difficult question since SO_3 is a highly reactive gas, and its concentration is generally two orders of magnitude lower than the SO_2 concentration. The SO_3 concentration can be measured online by the isopropanol absorption method; however, the reliability of the test results is relatively low. This work aims to find the error sources and to evaluate the extent of influence of each factor on the measurement results. The test results from a SO_3 analyzer showed that the measuring errors are mainly caused by the gas–liquid flow ratio, SO_2 oxidation, and the side reactions of SO_3. The error in the gas sampling rate is generally less than 13%. The isopropanol solution flow rate decreases 3% to 30% due to the volatilization of isopropanol, and accordingly, this will increase the apparent SO_3 concentration. The amount of SO_2 oxidation is linearly related to the SO_2 concentration. The side reactions of SO_3 reduce the selectivity of SO_4^{2-} to nearly 73%. As sampling temperature increases from 180 to 300°C, the selectivity of SO_4^{2-} decreases from 73% to 50%. The presence of H_2O in the sample gas helps to reduce the measurement error by inhibiting the volatilization of the isopropanol and weakening side reactions. A formula was established to modify the displayed value, and the measurement error was reduced from 25%–54% to less than 15%.
© 2017 The Research Center for Eco-Environmental Sciences, Chinese Academy of Sciences. Published by Elsevier B.V.

Introduction

In the combustion process of fossil fuels, a small fraction of sulfur is converted to sulfur trioxide (SO_3) (Bongartz and Ghoniem, 2015; Bongartz et al., 2015; Choudhury and Padak, 2016; Cordtz et al., 2013; Fleig et al., 2013; Wang et al., 2015). Flue gas SO_3 has undesirable effects on power plant operation due to plume opacity and corrosion problems (Fernando, 2003; Srivastava et al., 2004; Vainio et al., 2016). As the flue gas temperature drops in the air pre-heater, SO_3 starts to react with water vapor to form gaseous H_2SO_4 at a rapid rate. As flue gas

with 10 vol.% H_2O is cooled down from 400 to 200°C, approximately 8.7% and 99.3% of the SO_3 is respectively converted into gaseous H_2SO_4 on the assumption of approximate equilibrium (Hardman et al., 1998). The high boiling point of H_2SO_4 generates a high acid dew point for the gas phase. With 10 vol.% water vapor, the H_2SO_4 concentrations range from 1 to 50 ppmv, and the dew point varies from 116 to 154°C (Banchero and Verhoff, 1975). In this work, the term "SO_3" includes gaseous SO_3 and H_2SO_4. It is desirable to precisely measure the SO_3 concentration in the flue gas to limit equipment corrosion, heat loss, and acidic gas discharge. SO_3 measurement is difficult due to its

high reactivity, and can be hindered by: (1) comparatively low concentrations of SO_3 under typical conditions (Spellicy and Pisano, 2006; Blythe and Dombrowski, 2004), (2) interference from a high SO_2 concentration (Jaworowski and Mack, 1979), (3) losses of SO_3 by surface reactions or filter cake filtration (Belo et al., 2014; Cao et al., 2010; Galloway et al., 2015; Zhuang et al., 2011), and (4) SO_3 condensation (Guo et al., 2017).

The SO_3 measurement methods mainly include the controlled condensation method (CCM) and the isopropanol (IPA) absorption bottle method (Maddalone et al., 1979; Yang and Zheng, 2016). The CCM is the most-used technique, and is based on the condensation of H_2SO_4 above the water dew point and subsequent sulfate analysis. Maddalone et al. (1979) found that 95% of the injected H_2SO_4 could be recovered from a synthetic flue gas using the CCM with a coefficient of variance of ±6.7%. This method cannot be used to continuously measure SO_3 concentrations in flue gas online. The IPA absorption bottle method is based on the absorption of SO_3 in an 80 vol.% IPA solution diluted in water and sulfate analysis afterward. The main problem is interference by SO_2. The oxidation of a few parts per million of SO_2 dissolved in the IPA solution will result in a significant amount in proportion to the SO_3 concentration (Fleig et al., 2012). The dissolved SO_2 can be partially removed by bubbling air through the isopropanol solution.

The Pentol SO_3 analyzer (Pentol GmbH, Germany) based on the IPA method is a modified version of the Severn Science Analyzer designed by Jackson et al., and can be used to continuously measure SO_3 in flue gas online (Jackson et al., 1970, 1981). Typical values for the oxidation of SO_2 yield the equivalent of only 0.1 ppmv SO_3 for each 1000 ppmv SO_2 (Jackson et al., 1970). However, different researchers have obtained conflicting conclusions about the measurement errors. The results tested by Cooper at an Orimulsion-fired power plant showed that the SO_3 concentrations obtained with the Severn Science analyzer were 25 times higher than those obtained with the CCM (Cooper, 1995). An almost SO_3-free mixed gas containing air and 1000 ppmv SO_2 was tested by Fleig, and the results showed that less than 1 ppmv SO_3 was detected with the CCM, while a value of almost 10 ppmv SO_3 was obtained with the Pentol SO_3 analyzer (Fleig et al., 2012). A possible explanation is the oxidation of dissolved SO_2. It is worth noting that, initially, a gas stripping tube was used to remove dissolved SO_2 (Jackson et al., 1970). However, the gas stripping tube was removed from the current Pentol SO_3 analyzer. Koebel and Elsener (1997) obtained relatively lower SO_3 concentrations with the IPA drop method, for which the sampling process is similar to that of the Pentol SO_3 analyzer, and the explanation was that SO_3 may react with isopropanol, forming the monoester or diester of sulfuric acid. The gas sampling rate is controlled by a mass flow controller (MFC)

calibrated for nitrogen (N_2). Fleig et al. (2012) found that the actual gas sampling rate was lower due to the high CO_2 concentration under oxy-fuel fired conditions. An MFC correction factor for the flue-gas was calculated, and the reading of the Pentol SO_3 analyzer was divided by this correction factor (Fleig et al., 2012). In addition, volatilization loss of the IPA solution would lead to a positive deviation in measurement results (Barton and Mcadie, 1972).

In summary, the measurement errors of the SO_3 concentration mainly come from the measuring error of the gas sampling rate, IPA solution volatilization, the side reactions of SO_3 with isopropanol, and SO_2 oxidation. The aim of this work is to discover and evaluate the extent of influence of each factor on the measuring results, and then to reduce measuring errors by adjusting the process according to the influence factors. For the factors that cannot be controlled, correction coefficients are proposed to revise the measuring result.

1. Measurement principle and experiment platform

Both the sampling process and the analysis method for SO_3 are different between the Pentol SO_3 analyzer and the traditional IPA absorption bottle method. For the IPA absorption bottle method, flue gas is bubbled through an IPA absorption bottle which is placed in an ice water bath, wherein the SO_3 is absorbed. The SO_3 is stored in the IPA solution in the form of SO_4^{2-}, which is measured by titration with barium perchlorate using thorin as an indicator.

Compared with the IPA absorption bottle method, the advantage of the Pentol SO_3 analyzer is that it can achieve continuous online SO_3 measurement. The specific measurement principle is as follows. A simplified process diagram of the Pentol SO_3 analyzer is shown in Fig. 1. The flue gas continuously flows through a heated sampling probe and filter, and then contacts the IPA solution. Subsequently, the SO_3 in the flue gas is absorbed into the IPA solution as sulfate ions. As the solution passes through a bed of barium chloranilate, where reaction (1) occurs, and acidic chloranilate ions are formed. The acidic chloranilate ions absorb light preferentially at 535 nm as they pass through the optical cell continually, and then a series of voltages (U, mV) are output by the photometer. By maintaining a constant gas–liquid flow ratio (m), there is a near-exponential relationship between the SO_3 concentration (C_{SO3}, ppmv) and "U", as shown in Eq. (2).

$$SO_4^{2-} + BaC_6O_4Cl_2 + H^+ \rightarrow BaSO_4 + HC_6O_4Cl_2^- \tag{1}$$
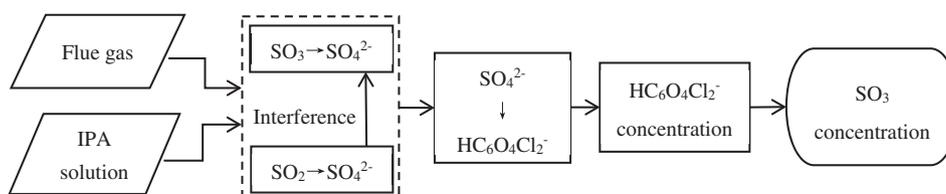
$$\log U = a \times m \times C_{SO3} + b \tag{2}$$

Fig. 1 – Simplified process diagram of the Pentol SO_3 analyzer. IPA: isopropanol.

Table 1 – Gas sampling rate and gas–liquid ratio "m".

Measurement range (ppmv)	Gas sampling rate (mL/min)	Gas–liquid flow ratio "m"
0–12.5	1000	1000
0–25	500	500
0–50	250	250
0–100	125	125

In the calibration process, the unknown parameters, a and b, can be calculated according to Eq. (2), since two voltage values are obtained by detecting two given calibration solutions equivalent to 5 and 45 ppmv of SO_3 in the sample gas as $m = 250$. In the measurement process, the unknown SO_3 concentrations in the flue gas are calculated using Eq. (2) through a series of voltage values. All the calculations are carried out by the analyzer. The IPA solution flow rate has a default value of 1 mL/min, while the gas sampling rate changes with the measurement range, as shown in Table 1.

If the instructions are strictly followed, the process of SO_4^{2-} converting to $HC_6O_4Cl_2^-$ and the detection of $HC_6O_4Cl_2^-$ is reliable (Jackson et al., 1981). Therefore, the gas sampling rate, IPA solution flow rate, oxidation of SO_2 and side reactions of SO_3 were further investigated in this work.

As shown in Fig. 2, the experimental platform consists of a flue gas simulation system, an SO_3 generation system and a Pentol SO_3 analyzer (Pentol GmbH, Germany). The flue gases are fed from cylinders and accurately controlled by mass flow controllers to provide mixed gases of varying SO_2, O_2 and N_2 contents. The water vapor is generated using a N_2 bubbling method. A sampling quartz tube, with a Y-type design and inner diameter of 2 mm, is placed in the top of the furnace, and its temperature is controlled individually. Two methods were used to generate SO_3. For the first method, SO_2 was catalytically oxidized on a V_2O_5/TiO_2 catalyst at 320°C to generate gaseous SO_3, with the mixed gas containing 1000 ppmv SO_2, 6% O_2 and a balance of N_2. If water vapor is simultaneously injected into the reactor, gaseous H_2SO_4 is generated. For the second method, a

dilute H_2SO_4 solution was gasified in a heated quartz tube to generate SO_3 mainly in the form of gaseous H_2SO_4, and the theoretical concentration of SO_3 was calculated by Eq. (3):

$$C_{SO3} = 22400Q_l \times C_{H2SO4}/Q \tag{3}$$

where C_{SO3} (ppmv) refers to the concentration of SO_3, C_{H2SO4} (mol/L) refers to the concentration of the H_2SO_4 solution, Q_l (μL/min) refers to the flow rate of the H_2SO_4 solution, and Q (mL/min) refers to the flow rate of the mixed gas (STP under dry conditions).

2. Results and discussion

2.1. Gas–liquid flow rate

The gas–liquid flow rates are the key factors affecting the measurement results. The gas sampling rate and IPA solution flow rate are independent and will be analyzed separately.

The gas sampling rate is controlled by a mass flow controller located downstream of the gas–liquid separator in the SO_3 analyzer. This mass flow controller is calibrated for nitrogen (N_2), therefore, multi-component flue gas will result in a deviation between the actual gas sampling rate (Q_g', mL/min) and the given gas sampling rate (Q_g, mL/min). In addition, a small portion of isopropanol volatilizes into the flue gas, which may exacerbate this deviation. Pure N_2 was sampled to measure Q_g' with an electronic soap film gas flow meter located upstream of the SO_3 analyzer. The ratio of Q_g' to Q_g is defined as the gas sampling rate coefficient (α), as shown in Eq. (4). The measurement results are shown in Fig. 3.

$$\alpha = Q_g'/Q_g \tag{4}$$

As shown in Fig. 3, Q_g' almost equals Q_g in the moderate measurement ranges of 0–50 and 0–25 ppmv, while obvious deviations emerge in the measurement ranges of 0–100 and 0–
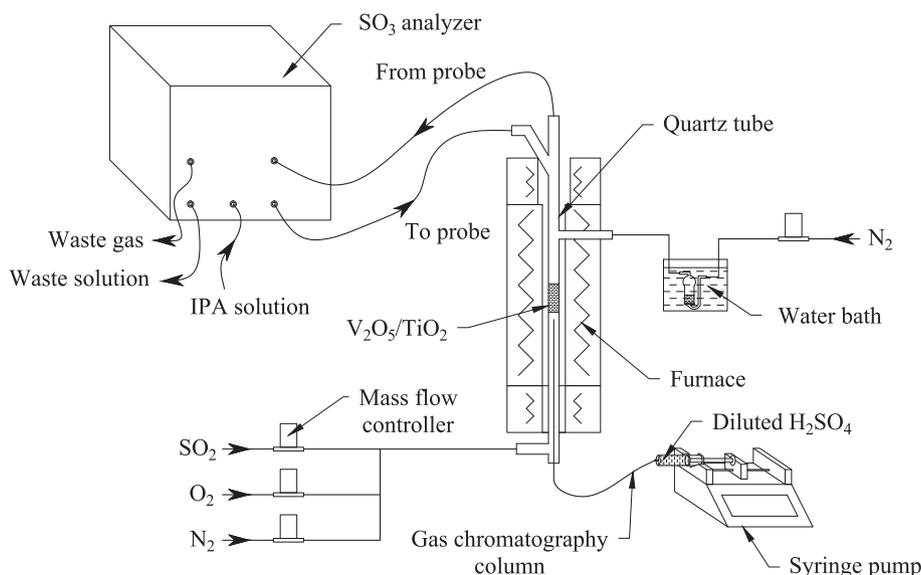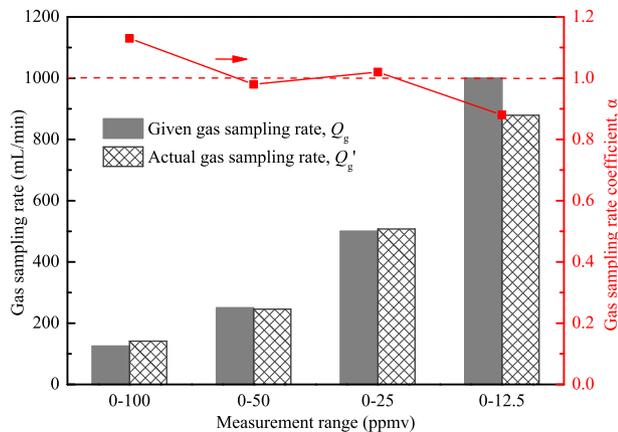

Fig. 2 – Experimental platform.

Fig. 3 – Gas sampling rates and gas sampling rate coefficient (α) in various measurement ranges.

12.5 ppmv. An "α" value of 1.13 means that the actual sampling rate is 13% higher than the given rate, and an "α" value of 0.88 indicates that the actual sampling rate is 12% lower than the given rate. Fleig et al. (2012) conducted the flue gas sampling using a Pentol SO_3 analyzer under oxy-fuel fired conditions and calculated a gas sampling rate coefficient of 0.76 due to a high CO_2 concentration. Therefore, it is necessary to measure Q_g' again when the gas composition and measurement range change. Since the SO_3 comes from the sample gas, the displayed value of the SO_3 concentration (C_{SO3}', ppmv) will increase with the gas sampling rate. When only the interference due to gas sampling rate is considered, the relationship among C_{SO3}, C_{SO3}' and "α" is shown in Eq. (5), and then C_{SO3}' can be corrected to C_{SO3} by Eq. (6).

$$\alpha = C_{SO3}'/C_{SO3} \tag{5}$$

$$C_{SO3} = C_{SO3}'/\alpha \tag{6}$$

In the process of flue gas and IPA solution concurrently flowing into the gas–liquid separator, the isopropanol migrates from the liquid phase to the gas phase. Based on the gas–liquid equilibrium, the maximal loss rate of the solution is 0.28 mL/min when the analyzer temperature is set to 30°C under the measurement range of 0–12.5 ppmv, while there is no solution volume loss when the water vapor content in flue gas is more than 25.5 vol.% (see Appendix A. Supplementary data). The water vapor content in coal-fired flue gas is usually less than 25.5 vol.%, so the actual IPA solution flow rate generally decreases in the sampling process.

The default value for the IPA solution flow rate (Q_{IPA}) generally is 1 mL/min; while the actual IPA solution flow rate (Q_{IPA}') is reduced due to the volatilization of the IPA solution. The ratio of Q_{IPA}' to Q_{IPA} is defined as the solution flow rate coefficient β, as shown in Eq. (7). The coefficient β is numerically equal to Q_{IPA}' because the default value of Q_{IPA} is 1.

$$\beta = Q_{IPA}'/Q_{IPA} \tag{7}$$

The volume of solution discharging from the "waste solution" outlet over a period of at least 30 min was measured to calculate the Q_{IPA}'. Two conditions were applied, including

a dry N_2 atmosphere and a wet N_2 atmosphere with 10 vol.% H_2O, with results shown in Fig. 4. In the dry atmosphere, the maximum Q_{IPA}' was 0.94 mL/min, and the minimum was 0.70 mL/min. In the wet atmosphere, the maximum Q_{IPA}' was 0.97 mL/min and the minimum was 0.85 mL/min. In the 0–12.5 ppmv range in the dry atmosphere, the loss of IPA solution reached a maximum of 0.30 mL/min, which is close to the calculated value of 0.28 mL/min (see Appendix A. Supplementary data). Therefore, the smaller the measurement range chosen, the larger the gas sampling rate and the greater the loss of IPA solution. The presence of water vapor can inhibit the volatilization of the solution, reducing the loss of IPA solution. The actual IPA solution flow rate decreases 3% to 30%, so that the displayed value of SO_3 concentration would increase 3% to 43%.

When the gas sampling rate is given, the SO_3 concentration in the IPA solution is inversely proportional to the IPA solution flow rate. Therefore, when only the interference due to solution volatilization is considered, the theoretical value, the displayed value and the coefficient β satisfy Eq. (8). C_{SO3}' can be corrected to C_{SO3} by Eq. (9).

$$\beta = C_{SO3}/C_{SO3}' \tag{8}$$

$$C_{SO3} = \beta \times C_{SO3}' \tag{9}$$

2.2. Oxidation of SO_2

In the IPA solution, SO_2 in the form of SO_3^{2-} is partially oxidized to SO_4^{2-}. The ratio of the amount of oxidized SO_2 (C_{ox}) and the original SO_2 concentration (C_{SO2}) in the flue gas is defined as the oxidation rate of SO_2, denoted as γ.

$$\gamma = C_{ox}/C_{SO2} \tag{10}$$

Some efforts have been made to eliminate the effect of SO_2. Gustavsson and Nyquist (2005) suggested bubbling air through the IPA solution to remove the dissolved SO_2. Jackson et al. (1970) used a gas stripping tube to remove dissolved SO_2 in the old version of the Pentol SO_3 analyzer, and typical values for
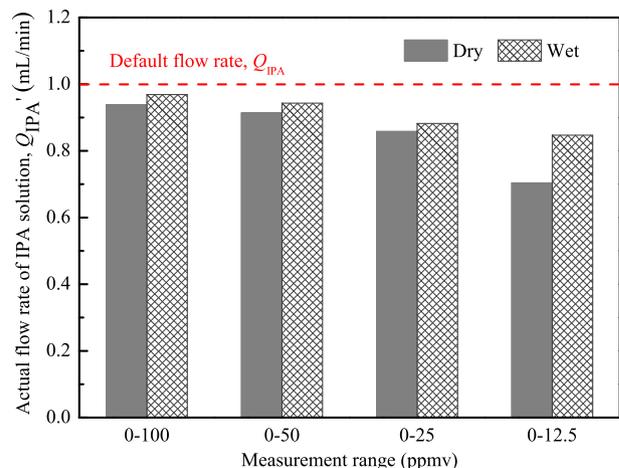

Fig. 4 – IPA solution flow rates in varied measurement ranges.

the oxidation of SO_2 yield the equivalent of only 0.1 ppmv SO_3 for each 1000 ppmv SO_2. However, the gas stripping tube was removed in the latest version of Pentol SO_3 analyzer. Therefore, it is necessary to investigate interference by SO_2.

An SO_3-free mixed gas, containing various SO_2 concentrations, 6% O_2 and a balance of N_2, was measured to evaluate the interference of SO_2 on the SO_3 measurement. The sampling tube and reaction tube were maintained at a room temperature of 20°C to minimize the oxidation of SO_2 in the gas phase as much as possible. The SO_3 concentrations were corrected by Eqs. (6) and (9), shown in Fig. 5. For the SO_3-free mixed gas, the displayed value of SO_3 concentration increased as the measurement range and SO_2 concentration increased. The detected SO_3 may come from the oxidation of SO_2 in the IPA solution and/or in the mixed gas cylinder, and the latter can be regarded as SO_3 impurities.

Based on Table 1, as the measurement range doubles, the gas sampling rate reduces by half, the total amount of SO_3 impurities (if any) in the gas phase entering the analyzer will also be halved, and then the amount of SO_4^{2-} in IPA solution will be halved, so that the displayed value of SO_3 concentration will not change. However, this deduction is contradictory to the experimental finding that the SO_3 concentration value approximately doubles as the measurement range doubles. Therefore, the detected SO_3 is not from SO_3 impurities in the gas phase.

Assuming that dissolution equilibrium is reached, the total amount of SO_2 dissolved in the IPA solution should be a constant when the SO_2 concentration in the gas phase is fixed. The passage time of the solution is also a constant since the solution flow rate is kept at 1 mL/min. So, the amount of generated SO_4^{2-} in the IPA solution will be a constant, and the displayed value of SO_3 concentration will double as the measurement range doubles due to the changing of the gas–liquid flow ratio (m). This deduction agrees with the experimental results; therefore, the detected SO_3 comes from the oxidation of SO_2.

Since the calibration solution was prepared as $m = 250$, the detected SO_3 from SO_3-free mixed gas in the range of 0–50 ppmv is numerically equal to the amount of oxidized SO_2, C_{ox}, as shown in Fig. 6. In the absence of O_2, the oxidation of SO_2 still occurs. The possible reason may be trace amounts of

O_2 dissolved in the IPA solution. In the presence of O_2, the dissolved O_2 in the IPA solution is relatively high, promoting the oxidation of SO_2. The presence of O_2 will increase the SO_3 concentration by approximately 1 ppmv. The SO_3 concentration increases approximately 1 ppmv as temperature increases from 20 to 200°C. High temperature also promotes the oxidation of SO_2.

The oxidation rate of SO_2, defined as "γ", is mainly affected by its own concentration. As the SO_2 concentration increases from 100 to 2000 ppmv, the "γ" decreases from approximately 3% to 0.4%, mainly ranging from 0.4% to 1.0%. The detected SO_3 concentration, ranging from 2.5 to 9.7 ppmv, shows a linearly positive relation to SO_2 concentration in the concentration range 100–2000 ppmv. A simple equation can be used to estimate the SO_3 concentration from the oxidation of SO_2, as shown in Eq. (11).

$$C_{ox} \approx 0.003 C_{SO2} + 2.9 \quad (C_{SO2} : 100\text{–}2000 \text{ ppmv}) \tag{11}$$

In summary, the oxidation of SO_2 is affected by SO_2 concentration, O_2 concentration and the sampling temperature. When only the interference due to SO_2 is considered, C_{SO3}, C_{SO3}' and C_{ox} follow Eq. (12). When SO_3 and SO_2 coexist in mixed gas, C_{ox} should be measured first under the experimental conditions, and then the SO_2 interference value should be subtracted from the displayed value.

$$C_{SO3} \approx C_{SO3}' - 250 C_{ox}/m \tag{12}$$

2.3. Side reactions of SO_3

In the sampling process, most SO_3 is dissolved in the IPA solution to form SO_4^{2-}, and the rest of the SO_3 is converted into by-products by side reactions. The molar ratio of SO_4^{2-} in the IPA solution ($n_{SO_4^{2-}}$) to SO_3 (n_{SO_3}) in the original flue gas is defined as the selectivity of SO_4^{2-}, denoted as "δ".

$$\delta = n_{SO_4^{2-}}/n_{SO_3} \tag{13}$$

During the calibration process, the IPA solution containing H_2SO_4 directly enters the reaction bed, which corresponds to a 100% selectivity of SO_4^{2-}. During the measurement process, the
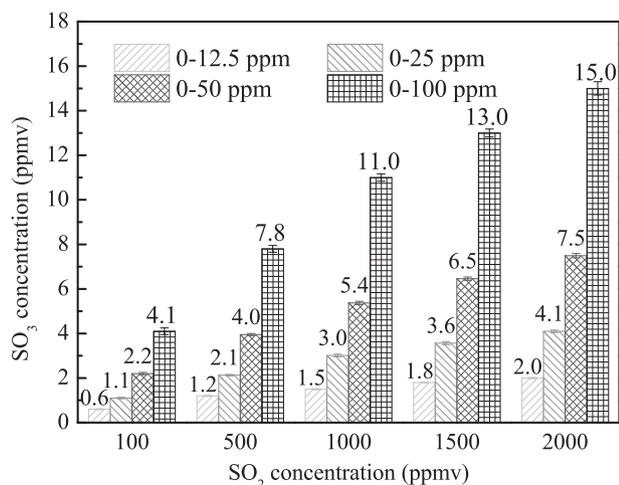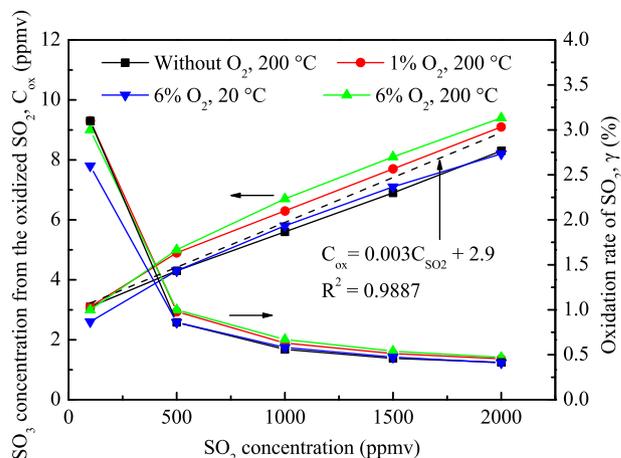

Fig. 5 – Interference due to SO_2 concentration.

Fig. 6 – Oxidation amount and oxidation rate of SO_2.

SO_3 is first absorbed by the IPA solution and then enters the reaction bed. At 200°C, SO_3 and isopropanol vapor coexist and may react to form undesirable by-products, similar to black carbon in this work. However, the by-products were found to be a sulfuric acid monoester or sulfuric acid diester in Koebel's research (Koebel and Elsener, 1997). This indicates that not all the SO_3 converts into SO_4^{2-} and that the "δ" is less than 100%.

To discover the effects of the chemical form of SO_3 on the measurement results, SO_3 was generated by the oxidation of SO_2 over V_2O_5/TiO_2 catalyst. Two cases were detected, including in the presence of H_2O or without H_2O. The sampling temperature was maintained at 200°C. Corrected by Eqs. (6), (9) and (12), the results are shown in Fig. 7. The gray area denotes a rough range of generated SO_3 concentrations gained by detecting the decrease of SO_2 concentration using a Fourier transform infrared (FTIR) spectrometer (Nicolet 6700, Thermo Fisher Scientific, USA) with a measurement error of ±1%. After introducing gaseous H_2O, the SO_3 concentration sharply increased from 2.5 to 27 ppmv. The result is consistent with the findings of Koebel and Elsener (1997). They modified the sampling process of the IPA drop method. Instead of contacting the IPA solution directly, the flue gas first came in contact with pure water, and immediately afterward with pure isopropanol. In this way side reactions are suppressed and almost all SO_3 in the sample is recovered. Essentially, highly active SO_3 is converted to relatively less active H_2SO_4 in the presence of H_2O, thus weakening the side reactions of SO_3. For detection of the SO_3 in sulfuric acid plant tail gas typically containing less than 60 ppmv $H_2O(g)$ (King et al., 2013), introducing gaseous H_2O should be considered.

By gasifying dilute H_2SO_4, 30 ppmv of SO_3 was prepared, wherein H_2SO_4 is the main form of SO_3 due to the presence of water vapor. The displayed value was corrected by Eqs. (6) and (9), and then the selectivity of SO_4^{2-} was calculated and shown in Fig. 8. The selectivity of SO_4^{2-} initially fluctuated around 73% from 180 to 210°C. As the temperature increased to 300°C, the selectivity of SO_4^{2-} gradually declined to 50% due to the increasingly intense side reactions. Therefore, the sampling temperature should be not higher than 210°C, while the temperature cannot be lower than the maximum acid dew point of 150°C under test conditions of 40 ppmv SO_3 and 10 vol.% H_2O. Taking into account a margin of safety, the proper sampling temperature range should be from 180 to 210°C.
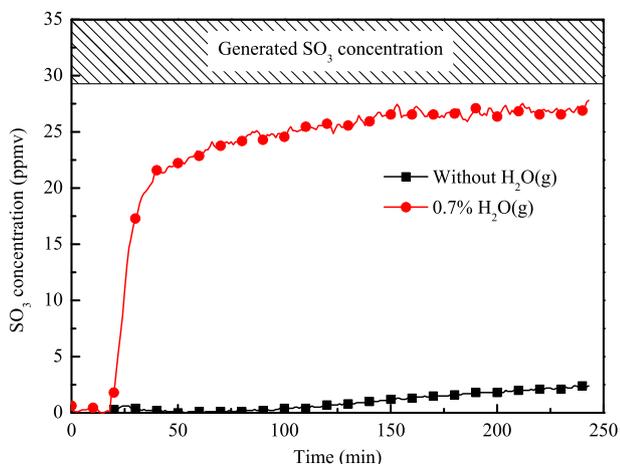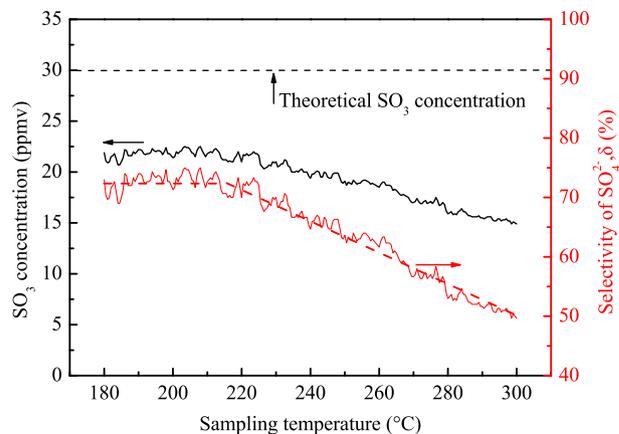

Fig. 8 – Influence of sampling temperature on the measurement of SO_3.

Mixed gases of 10, 20, 30, and 40 ppmv SO_3 were prepared by gasifying dilute sulfuric acid, and then measured at a sampling temperature of 200°C. After the SO_3 concentration was corrected by Eqs. (6) and (9), the average selectivity of SO_4^{2-} was approximately 73%, as shown in Fig. 9. The SO_3 concentration has no significant effect on the selectivity of SO_4^{2-}. The side reactions may also be considered by the Pentol SO_3 analyzer, since it was found that during the calibration process, calibration solutions equivalent to 4.75 and 42.75 ppmv of SO_3 in the sample gas were used to calibrate the points of 5 and 45 ppmv. The difference may imply that the average selectivity of SO_4^{2-} is 95% when the original sampling probe is used. The higher selectivity may be due to the proper structural design of the probe, which weakens side reactions.

The side reactions result in a decrease in SO_4^{2-} selectivity, while low temperature and the presence of H_2O can significantly weaken the side reactions. When only the interference due to side reactions is considered, Eq. (14) can be used to calculate the selectivity of SO_4^{2-}, and C_{SO3}' can be corrected by Eq. (15).

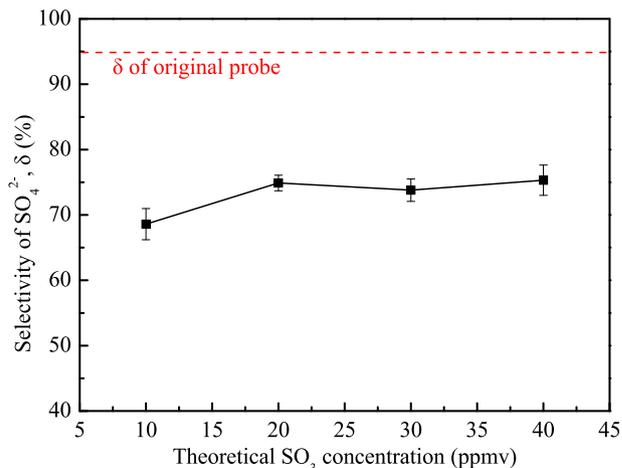$$\delta = C_{SO3}'/C_{SO3} \qquad (14)$$

Fig. 7 – Influence of H_2O on SO_3 concentration.

Fig. 9 – Influence of SO_3 concentration on the selectivity of SO_4^{2-}.

$$C_{SO3} = C_{SO3}'/\delta \qquad (15)$$

2.4. Measurement error analysis

As summarized in Table 2, the measurement errors of the SO_3 concentration mainly come from the gas sampling rate, IPA solution flow rate, SO_2 oxidation and the side reactions of SO_3 with isopropanol. The measurement error caused by the above four factors can be partially eliminated by formula correction, and the correction is as follows:

$$C_{SO3}{''} \approx (C_{SO3}' - 250C_{ox}/m) \times \beta/(\alpha \times \delta) \qquad (16)$$

$C_{SO3}{''}$ is the corrected SO_3 concentration. Before the experiment, the sampling gas flow rate coefficient (α), IPA solution flow rate coefficient (β), oxidation amount of SO_2 (C_{ox}) and the selectivity of SO_4^{2-} (δ) should be measured. In the laboratory, these parameters can be measured easily. In the plant, in addition to the above factors, SO_3 adsorption on the filter cake also affects the measurement results. Eq. (16) is not sufficient to correct the plant test results, but it can still reduce the measurement error.

In this work, the displayed value of SO_3 concentration was corrected by Eq. (16), and Fig. 10 shows the theoretical value (C_{SO3}), the displayed value (C_{SO3}') and the corrected value ($C_{SO3}{''}$). The displayed value is lower than the theoretical value by approximately 25% to 54%. The corrected value is 15% lower than the theoretical value at the SO_3 concentration of 10 ppmv, in that the measurement error is larger at lower concentrations. $C_{SO3}{''}/C_{SO3}$ is closest to 1 and the relative error is less than 5% for SO_3 concentrations more than 20 ppmv. The correction of the displayed value using Eq. (16) can significantly reduce the detection error.

3. Conclusions

The measurement errors for the SO_3 concentration mainly result from the gas–liquid flow rate, the side reactions of SO_3 and SO_2 oxidation. The errors in the gas sampling rate and IPA
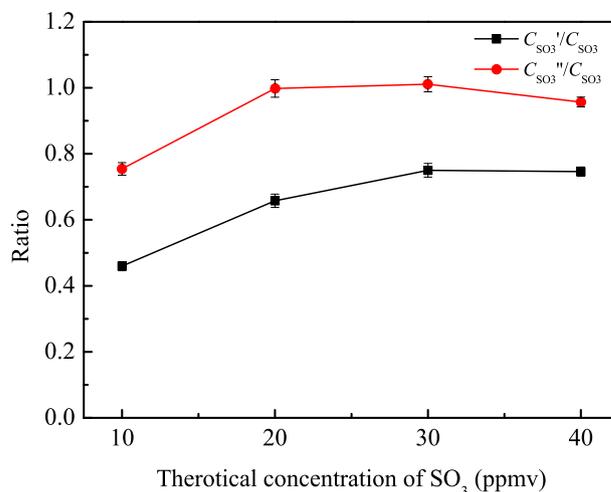

Fig. 10 – Comparison of theoretical concentration of SO_3 (C_{SO3}), displayed concentration of SO_3 (C_{SO3}'), and correction concentration of SO_3 ($C_{SO3}{''}$).

solution flow rate are rooted in the instrument, while the oxidation of SO_2 and the side reactions lie in the properties of SO_2 and SO_3. The error in the gas sampling rate is generally less than 13%. The isopropanol solution flow rate decreases 3%–30% due to the volatilization of isopropanol, which accordingly increases the SO_3 concentration. The oxidation of SO_2 interferes with the SO_3 measurement, and the oxidation amount is linearly related to the SO_2 concentration. The side reactions between SO_3 and the IPA solution reduce the selectivity of SO_4^{2-}. Relatively low sampling temperature and the presence of water vapor help to reduce the measurement error through inhibiting side reactions. A formula was proposed to correct the displayed value, which can reduce the measurement error from 25%–54% to less than 15%. The results of this work provide a useful reference for SO_3 measurement using the online isopropanol absorption method.

Table 2 – Error sources and correction methods for measurement error.

Error sources	Coefficient	Value[*]	Error of C_{SO3}'[*]	Correction method
Gas sampling rate	α	0.88–1.13 (–)	−12%–13%	C_{SO3}'/α
Isopropanol (IPA) solution flow rate	β	0.70–0.97 (–)	3%–43%	$\beta \times C_{SO3}'$
Side reactions of SO_3	δ	0.50–0.75 (–)	−50%–−25%	C_{SO3}'/δ
Oxidation of SO_2	C_{ox}	2.5–9.7 (ppmv)	0.6–15.0 (ppmv)	$C_{SO3}' - 250C_{ox}/m$

C_{SO3}': displayed concentration of SO_3; α: gas sampling rate coefficient; β: solution flow rate coefficient; δ: selectivity of SO_4^{2-}; C_{ox}: SO_3 concentration from the oxidized SO_2.
– means that the parameters are dimensionless.
[*] Experimental conditions: 100–2000 ppmv SO_2, $O_2 \leq 6\%$, $H_2O \leq 10\%$, 10–40 ppmv SO_3, N_2 as a balance gas, and sampling temperature $\leq 300°C$.

Acknowledgments

Appendix A. Supplementary data

Supplementary data to this article can be found online at https://doi.org/10.1016/j.jes.2017.11.026.

REFERENCES

Banchero, J.T., Verhoff, F.H., 1975. Evaluation and interpretation of vapor-pressure data for sulfuric-acid aqueous-solutions with application to flue gas dew points. J. Inst. Fuel 48, 76–80.

Barton, S.C., Mcadie, H.G., 1972. A specific method for the automatic determination of ambient H_2SO_4 aerosol. [C]// Proceedings of Second International Clean Air Congress, pp. 379–382.

Belo, L.P., Spörl, R., Shah, K.V., Elliott, L.K., Stanger, R.J., Maier, J., et al., 2014. Sulfur capture by fly ash in air and oxy-fuel pulverized fuel combustion. Energy Fuel 28, 5472–5479.

Blythe, G., Dombrowski, K., 2004. SO_3 Mitigation Guide Update. EPRI, Palo Alto, CA (2004. 1004168).

Bongartz, D., Ghoniem, A.F., 2015. Impact of sour gas composition on ignition delay and burning velocity in air and oxy-fuel combustion. Combust. Flame 162, 2749–2757.

Bongartz, D., Shanbhogue, S.J., Ghoniem, A.F., 2015. Formation and control of sulfur oxides in sour gas oxy-combustion: prediction using a reactor network model. Energy Fuel 29, 7670–7680.

Cao, Y., Zhou, H.C., Jiang, W., Chen, C.W., Pan, W.P., 2010. Studies of the fate of sulfur trioxide in coal-fired utility boilers based on modified selected condensation methods. Environ. Sci. Technol. 44, 3429–3434.

Choudhury, N.N., Padak, B., 2016. A comprehensive experimental and modeling study of sulfur trioxide formation in oxy-fuel combustion international. Int. J. Greenhouse Gas Control 51, 165–175.

Cooper, D., 1995. Optimisation of a NaCl adsorbent tube method for SO_3 measurements in combustion flue gases. IVL, Institutet for Vatten-och Luftvardsforskning. Swedish Environmental Research Institute.

Cordtz, R., Schramm, J., Rabe, R., 2013. Investigating SO_3 formation from the combustion of heavy fuel oil in a four-stroke medium-speed test engine. Energy Fuel 27, 6279–6286.

Fernando, R., 2003. SO_3 Issues for Coal-Fired Plant. IEA Coal Research.

Fleig, D., Vainio, E., Andersson, K., Brink, A., Johnsson, F., Hupa, M., 2012. Evaluation of SO_3 measurement techniques in air and oxy-fuel combustion. Energy Fuel 26, 5537–5549.

Fleig, D., Alzueta, M.U., Normann, F., Abián, M., Andersson, K., Johnsson, F., 2013. Measurement and modeling of sulfur trioxide formation in a flow reactor under post-flame conditions. Combust. Flame 160, 1142–1151.

Galloway, B.D., Sasmaz, E., Padak, B., 2015. Binding of SO_3 to fly ash components: CaO, MgO, Na_2O and K_2O. Fuel 145, 79–83.

Guo, B.Y., Yang, D., Su, Y.B., Yu, A.B., 2017. Process modelling of low temperature electrostatic precipitators. Powder Technol. 314, 567–576.

Gustavsson, L., Nyquist, G., 2005. Värmeforsks Mäthandbok. Värmeforsk Service AB, Stockholm (in Swedish).

Hardman, R., Stacy, R., Dismukes, E., 1998. Estimating sulfuric acid aerosol emissions from coal-fired power plants. DOE-FETC Conference on Formation, Distribution, Impact, and Fate of Sulfur Trioxide in Utility Flue Gas Streams, Pittsburgh, PA.

Jackson, P.J., Langdon, W.E., Reynolds, P.J., 1970. Automatic continuous measurement of sulphur trioxide in flue gases. J. Inst. Fuel 43, 10–17.

Jackson, P.J., Hilton, D.A., Buddery, J.H., 1981. The prevention of acid smuts.5. Continuous measurement of sulfuric-acid vapor in combustion gases using a portable automatic monitor. J. Inst. Energy 54, 124–135.

Jaworowski, R.J., Mack, S.S., 1979. Evaluation of methods for measurement of SO_3/H_2SO_4 in flue gas. J. Air Pollut. Control Assoc. 29, 43–46.

King, M., Moats, M., Davenport, W.G., 2013. Sulfuric Acid Manufacture: Analysis, Control and Optimization. 2nd edn. Elsevier, Newnes, pp. 325–340.

Koebel, M., Elsener, M., 1997. Determination of sulfur trioxide in flue gases using isopropyl alcohol as an absorbant - a critical investigation. Gefahrstoffe - Reinhalt. Luft 57, 193–199.

Maddalone, R.F., Newton, S.F., Rhudy, R.G., Statnick, R.M., 1979. Laboratory and field evaluation of the controlled condensation system for SO_3 measurements in flue gas streams. J. Air Pollut. Control Assoc. 29, 626–631.

Spellicy, R., Pisano, J., 2006. Continuous Measurement of SO_3 in a Coal-Fired Power Plant. EPRI, Palo Alto, CA, p. 1010375.

Srivastava, R.K., Miller, C.A., Erickson, C., Jambhekar, R., 2004. Emissions of sulfur trioxide from coal-fired power plants. J. Air Waste Manage. Assoc. 54, 750–762.

Vainio, E., Kinnunen, H., Lauren, T., Brink, A., Yrjas, P., DeMartini, N., et al., 2016. Low-temperature corrosion in co-combustion of biomass and solid recovered fuels. Fuel 184, 957–965.

Wang, X., Liu, X., Li, D., Zhang, Y., Xu, M., 2015. Effect of steam and sulfur dioxide on sulfur trioxide formation during oxy-fuel combustion. Int. J. Greenhouse Gas Control 43, 1–9.

Yang, D., Zheng, F., 2016. Detection technique of SO_3 content in coal-fired flue gas and accuracy analysis. Clean Coal Technology and Sustainable Development: Proceedings of the 8th International Symposium on Coal Combustion, pp. 563–566.

Zhuang, Y., Martin, C., Pavlish, J., Botha, F., 2011. Cobenefit of SO_3 reduction on mercury capture with activated carbon in coal flue gas. Fuel 90, 2998–3006.